

Lawrence Berkeley National Laboratory

Recent Work

Title

STUDY OF THE REACTIONS $\text{Pr}^{141}(\text{C}^{12}, \text{lin})\text{Tb}^{149}$ AND $\text{Te}^{130}(\text{C}^{12}, \text{j}5\text{n})\text{Ce}^{137\text{m}}$ BY MEANS OF RECOIL TECHNIQUES

Permalink

<https://escholarship.org/uc/item/3cm2b24k>

Authors

Morton, John R.
Choppin, Gregory R.
Harvey, Bernard G.

Publication Date

1962-01-24

University of California

Ernest O. Lawrence
Radiation Laboratory

TWO-WEEK LOAN COPY

*This is a Library Circulating Copy
which may be borrowed for two weeks.
For a personal retention copy, call
Tech. Info. Division, Ext. 5545*

Berkeley, California

DISCLAIMER

This document was prepared as an account of work sponsored by the United States Government. While this document is believed to contain correct information, neither the United States Government nor any agency thereof, nor the Regents of the University of California, nor any of their employees, makes any warranty, express or implied, or assumes any legal responsibility for the accuracy, completeness, or usefulness of any information, apparatus, product, or process disclosed, or represents that its use would not infringe privately owned rights. Reference herein to any specific commercial product, process, or service by its trade name, trademark, manufacturer, or otherwise, does not necessarily constitute or imply its endorsement, recommendation, or favoring by the United States Government or any agency thereof, or the Regents of the University of California. The views and opinions of authors expressed herein do not necessarily state or reflect those of the United States Government or any agency thereof or the Regents of the University of California.

UNIVERSITY OF CALIFORNIA
Lawrence Radiation Laboratory
Berkeley, California

Contract No. W-7405-eng-48

STUDY OF THE REACTIONS $\text{Pr}^{141}(\text{C}^{12}, 4n)\text{Tb}^{149}$ AND
 $\text{Te}^{130}(\text{C}^{12}, 5n)\text{Ce}^{137m}$ BY MEANS OF RECOIL TECHNIQUES

John R. Morton III

Gregory R. Choppin

Bernard G. Harvey

January 24, 1962

Study of the Reactions $\text{Pr}^{141}(\text{C}^{12}, 4n)\text{Tb}^{149}$ and
 $\text{Te}^{130}(\text{C}^{12}, 5n)\text{Ce}^{137\text{m}}$ by Means of Recoil Techniques

John R. Morton III, Gregory R. Choppin, and Bernard G. Harvey

Lawrence Radiation Laboratory

University of California

Berkeley, California

January 24, 1962

ABSTRACT

The reactions $\text{Pr}^{141}(\text{C}^{12}, 4n)\text{Tb}^{149}$ and $\text{Te}^{130}(\text{C}^{12}, 5n)\text{Ce}^{137\text{m}}$ were examined by means of recoil techniques. The experimental angular distributions were compared with distributions calculated by a Monte Carlo method, based upon the compound nucleus and statistical models, with a neutron angular distribution of the form $W(\theta) d\Omega = (A + B \cos^2 \theta) d\Omega$. The results from the $\text{Pr}^{141}(\text{C}^{12}, 4n)$ reaction are in agreement with the simple theory. The $\text{Te}^{130}(\text{C}^{12}, 5n)$ data can be explained by formation of a compound nucleus which de-excites with enhanced probability for gamma emission.

Study of the Reactions $\text{Pr}^{141}(\text{C}^{12}, 4\text{n})\text{Tb}^{149}$ and
 $\text{Te}^{130}(\text{C}^{12}, 5\text{n})\text{Ce}^{137\text{m}}$ by Means of Recoil Techniques*

John R. Morton III,^{††} Gregory R. Choppin,[§] and Bernard G. Harvey

Lawrence Radiation Laboratory

University of California

Berkeley, California

January 24, 1962

INTRODUCTION

The method of deducing information about nuclear reaction mechanisms from study of the ranges and angular distributions of the recoiling residual nuclei has been previously described.^{1,2,3} The ranges of the recoils distinguish compound nucleus reactions from direct reactions, for in the former case the mean range corresponds to a mean momentum equal to that of the incident particle. The angular distribution of recoils from a compound nucleus reaction is a function only of the angular distribution and momentum spectrum of the evaporated particles, of the momentum of the incident particle, and of the mass of the target nucleus.

In previous work^{1,2,3} it was found that several nuclear reactions induced by helium ions in the energy range 20-48 Mev gave recoil angular distributions in excellent agreement with the simplest evaporation model. In particular, the model assumed that as long as the excitation energy of the compound system exceeded the binding energy of a neutron, then a neutron would indeed be evaporated. Emission of γ quanta was assumed to be of negligible importance as long as particle evaporation was energetically possible.

In heavy-ion-induced reactions, however, the angular momentum of the compound nucleus may attain such large values that this simple picture must be modified. The level density of states of sufficiently high spin may be so low near the end of the evaporation chain that neutron evaporation becomes difficult. In addition a substantial amount of energy may be stored in collective modes (rotations and vibrations) whose quadrupole γ -decay rates are enhanced. In either case, the result may be that a substantially greater fraction of the excitation energy appears as photons. Since the momenta of these photons are much smaller than that of a neutron removing the same amount of excitation energy, the angular distribution of the recoil nuclei should be narrower (i. e. , closer to the direction of the incident particles).

The reaction $\text{Te}^{130}(\text{C}^{12}, 5n)\text{Ce}^{137m}$ was studied because Choppin and co-workers^{4,5} had previously found some anomalies in its excitation function which suggested that a substantial amount of energy was indeed carried away by γ rays.

EXPERIMENTAL PROCEDURES

Recoil Angular Distribution Experiments

The praseodymium targets and the natural tellurium targets were prepared by vacuum evaporation of the metal onto 0.00025-in. aluminum foils. The Te^{130} targets were prepared by electroplating enriched Te^{130} onto gold foils 0.0001 in. thick.⁵ In each case the thickness of the deposit was determined by weighing. The Pr^{141} target deposits were 24.6 ± 5.0 $\mu\text{g}/\text{cm}^2$ thick. The Te^{130} targets ranged from 10 to 30 $\mu\text{g}/\text{cm}^2$, with uncertainties of about 5 $\mu\text{g}/\text{cm}^2$. The natural tellurium targets used for the range experiments contained 240 $\mu\text{g}/\text{cm}^2$ of the target material.

All the bombardments were done at the heavy-ion linear accelerator (HILAC). The particle-beam energies were adjusted through use of aluminum degrading foils according to the range-energy data of Walton,⁶ which are also consistent with the published data of Northcliffe.⁷

The recoil angular distribution experiments followed the technique described in ref. 1, in which the recoils impacted into a circular catcher foil placed behind the target in an evacuated chamber. After the bombardment, the catcher was sectioned into concentric circles. The yield of product from the $\text{Pr}^{141}(\text{C}^{12}, 4n)\text{Tb}^{149}$ reaction was determined by direct count of the gross alpha activities and by alpha pulse height analysis. The yield of product from the $\text{Te}^{130}(\text{C}^{12}, 5n)\text{Ce}^{137\text{m}}$ reaction was determined by counting the conversion electron activity from the radiochemically separated cerium. The cerium data were corrected for chemical yield, and self-absorption corrections based upon data from $\text{Ba}^{135\text{m}}$ were applied.⁸

Recoil Range Experiments

The recoil range experiments used a differential range technique in which the stopping medium was a stack of aluminum leaf with surface densities in the range 164-169 $\mu\text{g}/\text{cm}^2$. An abbreviated chemical separation was used to permit a determination of the combined cerium and lanthanum product yields.

MONTE CARLO CALCULATIONS

Calculation of the angular distribution of the recoiling residual nuclei from nuclear reactions has been discussed at some length.¹⁻³ The previous treatments have followed the compound nucleus and statistical models and assumed that neutrons are evaporated isotropically from the compound nucleus with an energy spectrum of the form

$$P(E_n) dE_n = E_n e^{-E_n/T} dE_n \quad (1)$$

The parameter T was considered to be constant for the emission of successive neutrons along the evaporation chain.

The calculations described here differ from the previous ones in two respects:

(1) The maximum excitation energy available as kinetic energy is given by $E_{p(c.m.)} + Q_n - E_\gamma$, where $E_{p(c.m.)}$ is the energy of the projectile particle in the center-of-mass system, Q_n is the Q for the reaction in which n neutrons are emitted, and E_γ represents some portion of the excitation energy not available as kinetic energy for the neutrons. With this single modification in the energetics, the neutron energies were selected randomly by the procedure of ref. 3.

(2) The neutrons were assumed to be evaporated from the recoiling nucleus in a distribution of the form

$$W(\theta) d\Omega = (A + B \cos^2 \theta) d\Omega, \quad (2)$$

where $W(\theta)$ is the probability of having a polar angle between θ and $\theta + d\theta$, and A and B are parameters.

The scheme for obtaining random values of θ , weighted by the distribution of Eq. (2), is similar to that for selecting the neutron energies except the range of probabilities is the same for successive neutrons. An integral probability function is obtained by integrating (2) to give

$$R = [A \cos \theta + (B/3) \cos^3 \theta] + A + B/3, \quad (3)$$

where R is an integral probability function, illustrated graphically in Fig.

This expression is difficult to solve explicitly for a unique θ from a randomly chosen value for R , so a 2049-space table was set up for $R[(N - 1) \Delta\theta]$, where $\Delta\theta$ was $\pi/2048$. A randomly selected value for R could then be associated with a value for θ . The random value for R was obtained by multiplying the maximum value for R , $2(A + B/3)$, by a random number between 0 and 1. The random value was located in the R table between $R(N)$ and $R(N - 1)$. The corresponding chosen value for θ for the i th neutron was

$$\theta_i = (N - 1) \Delta\theta. \quad (4)$$

The azimuthal angles ϕ_i were obtained by multiplying 2π by a random number between 0 and 1. Random values for θ and ϕ were obtained for each neutron for which an energy had been selected.

The neutron momenta were summed by taking successive projections on the Cartesian coordinates using the relations

$$P_{x,i} = P_{x,i-1} + P_i \sin \theta_i \cos \phi_i, \quad (5)$$

$$P_{y,i} = P_{y,i-1} + P_i \sin \theta_i \sin \phi_i, \quad (6)$$

$$P_{z,i} = P_{z,i-1} + P_i \cos \theta_i. \quad (7)$$

The final resultant momentum is

$$P_r = [P_x^2 + P_y^2 + P_z^2]^{1/2}, \quad (8)$$

and its polar angle in the system of the recoiling nucleus is

$$\theta_r = \cos^{-1} (P_z / P_r). \quad (9)$$

The angle the recoiling nucleus makes with the beam axis in the laboratory system is

$$\Theta = \tan^{-1} \left[\frac{(1 - \cos^2 \theta_i)^{\frac{1}{2}}}{(\cos \theta_i + P_a/P_n)} \right], \quad (10)$$

where P_a and P_n are respectively the momentum of the projectile particle and the resultant momentum for i neutrons, and θ is the angle between P_n and the beam axis in the system of the recoiling nucleus.

The Monte Carlo calculations were performed on the IBM 704 computer. Normally, the calculations were made for 5000 to 10,000 cases of the reaction of interest.

The computations produced the following items of information:

(a) The number of recoil events for the reaction of interest, corrected for solid angle, in angular increments corresponding to a given combination of target-to-catcher distance and ring radii. The calculated distributions are shown in Figs. 2 and 3.

(b) The total number of each type of neutron evaporation reaction that occurred.

In addition, the following information was obtained optionally:

(a') The neutron angular distribution in the system of the recoiling nucleus in angular intervals of $\pi/10$ radian. Figure 4 shows how the large mesh size (increment of angle) used in printing out the data leads to some distortion of the actual neutron angular distribution — an apparent flattening for the forward and backward angles. Representative neutron angular distributions are shown in Fig. 5.

(b') The energy spectra of each of the emitted neutrons for the reaction of interest in energy intervals of 0.2 Mev. Figures 6 and 7 show some representative neutron energy distributions.

The information above permitted several conclusions about the various parameters of the Monte Carlo calculations. Their effects are presented below in terms of their influence on the magnitude of $W(1/2)$, the angle at which the distribution falls to half its value at 0 degrees:

1. Anisotropy

Figure 8 shows that the calculations are fairly insensitive to the value of B/A . Up to $B/A \approx 0.2$ for C^{12} reactions and $B/A \approx 1.0$ for alpha-induced reactions, the $W(1/2)$ values do not depart appreciably from those expected from an isotropic distribution for evaporated neutrons. Hence it is apparent that agreement of experimental distributions with a calculation of this type is not necessarily indicative of neutron emission according to precise values for B/A ; moderate ranges of anisotropy could not be distinguished from the isotropic case. Also, isotropy of neutron emission could not be established by this means.

It is recognized, of course, that a distribution of the form $A + B \cos^2 \theta$ is incapable of representing strong forward-backward anisotropies. For such cases, the form $(\sin \theta)^{-1}$ is more appropriate^{9,10}; however, the $(\sin \theta)^{-1}$ distribution is not considered to be applicable in this case.^{9,11}

2. Nuclear Temperature

Figure 9 shows that the shape of the calculated recoil angular distribution is much less sensitive to the value of T in the reactions considered here than it was for one of the reactions previously studied. For a reaction in which neutron evaporation proceeds as long as the residual excitation energy exceeds the binding energy of the next neutron, the total kinetic energy of the neutrons, regardless of the value of T , must lie in the range $(E^* + Q)$ to $(E^* + Q - B)$. E^* is the center-of-mass kinetic energy of the incident

particle, Q is the (negative) Q value of the reaction, and B is the binding energy of the next neutron. The parameter T determines only the way in which this energy is shared between successive neutrons of the evaporation chain, and where in the permitted range the most probable total neutron kinetic energy will lie. Hence the parameter T can have only little effect on the neutron momenta (and hence on the angular distribution of the recoils) when $(E^* + Q)$ is much greater than B . In the present work, $(E^* + Q)$ was typically 15-40 Mev, whereas B was about 7 Mev; therefore, the assumption of constant nuclear temperature is not unreasonable for this purpose, although, in general, such an assumption is not believed to be valid.¹²⁻¹⁴

3. Excitation Not Removed by Neutron Emission: E_γ

The sensitivity to the parameter E_γ is shown in Fig. 10. It is perhaps physically unreasonable to use a single value rather than some distribution of values for this quantity in a given calculation. This was done arbitrarily to avoid undue complexity. It is believed that this assumption may cause the calculated recoil angular distributions to be unrealistically narrowed near θ_{\max} ; however, at angles from 0 to the neighborhood of $W(1/2)$, the more probable values from a distribution should dominate.

4. Effect of Angular Resolution

Figure 4 shows the extreme distortion that can be caused by use of a very coarse angular mesh size in printing out the neutron angular distributions. The effect of angular resolution was also considered for the recoil angular distribution; in this case the angular increments were much smaller.^{15,16} Calculations were performed for target-to-catcher spacings of 4.0 and 10.0 cm with other conditions unchanged; this corresponds to a reduction in the angular mesh by a factor of 2.5. This change produced

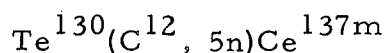
improvement in angular resolution at small angles, but the recoil angular distributions defined by each set of points were essentially identical. This means that moderate variations in the mesh size are not particularly important. In practically every case, calculations were compared with experiments having the same angular resolution.

RESULTS

The recoil angular distributions calculated by the Monte Carlo method may be compared with experiment. Agreement between calculations and experiment lends support to the compound-nucleus/statistical-model description of these reactions. The recoil range measurements provide more direct information about the extent of momentum transfer. Normally, formation of a compound nucleus is expected to lead to recoiling products with the maximum attainable kinetic energy although a few exceptions have been reported.¹⁷ The range of the recoils is known to be an increasing function of their energy.¹⁸

The calculated and the experimental recoil angular distributions are compared below, both directly and in summary plots of $W(1/2)$ vs $(E_{p(c.m.)} + Q)$, the energy available to evaporated neutrons. Agreement between the distributions is judged by a detailed comparison of the two distributions from 0 degrees to angles in the neighborhood of $W(1/2)$. The departure of the experimental points from the smooth curve at wider angles is attributed to scattering from the surface of the target or from gas molecules in the evacuated chamber.

The recoil angular distribution and range results follow, grouped together for each particular set of reactions.



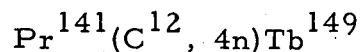
In Figs. 2 and 11 the experimental distributions are compared with calculated ones for the isotropic case, and for the nonisotropic case where best fits are obtained by using $B/A = 1.2$ and various combinations of T and E_y , listed in Table I. Selection of the value for B/A is discussed later. The experimental angular-distribution data are listed in Table II.

A typical histogram for the recoil range data from natural $\text{Te} + \text{C}^{12}$ is given in Fig. 12. The Gaussian fit by the probability plot is given in Fig. 13 for the same set of data.

The recoil range data are compared in Fig. 14 with a range-energy curve calculated for Ce recoils by adjusting the published values for Tb^{149} for differences in Z and A .¹⁹ The values for the recoil energies are calculated by assuming formation of a compound nucleus. The experimental recoil range data are summarized in Table III. The quantity ρ is the "straggling parameter"²⁰ for the recoil range distribution, defined by

$$\rho = \left[\frac{2A_s A_r}{3(A_s + A_r)^2} \right]^{\frac{1}{2}} \quad (11)$$

A_s and A_r represent the atomic mass numbers of the stopping medium and recoil.



The experimental and Monte Carlo recoil angular distributions are compared in Figs. 3 and 15. The experimental data are summarized in Table IV.

Excellent recoil range data for this reaction have been published by Winsberg and Alexander.¹⁹

DISCUSSION

The recoil angular distribution and range data listed in the preceding section, together with the experimental excitation functions, furnish fairly direct information about many features of the nuclear reaction mechanisms.

1. Pr¹⁴¹(C¹², 4n)Tb¹⁴⁹

Figures 3 and 15 show that the experimental recoil angular distributions agree quite closely with the simple isotropic Monte Carlo calculation using $E_{\gamma} = 0$ and $T = 1.5$ Mev. This value for T was calculated from Alexander's experimental excitation function,²¹ using the evaporation model of Jackson.²² It was shown in Fig. 9 that the precise choice for T should not be critical for the result of the Monte Carlo calculation.

The maximum measured cross section for this reaction is about 35 mb.²¹

Recoil range data for Tb¹⁴⁹ from this and a number of other reactions have recently been published by Winsberg and Alexander.¹⁹ Their analysis shows that the recoil range results for this reaction are consistent with compound-nucleus formation.

Agreement of the recoil angular distribution data with the calculations reinforces the conclusions about compound-nucleus formation, and further suggests that the compound system de-excites primarily by evaporation of neutrons having energy spectra similar to the form of Eq. (1). The agreement between the experimental and calculated distributions also suggests that there is no very great angular anisotropy in the neutron evaporation.

2. $\text{Te}^{130}(\text{C}^{12}, 5\text{n})\text{Ce}^{137\text{m}}$

Figure 14 shows that the recoil ranges from the natural Te agree reasonably well with the ranges calculated from the Tb^{149} data. This is fairly convincing evidence for the formation of a compound nucleus. We suspect that the slight displacement of the points is caused by some systematic difference in experimental technique. If one neutron from the bombarding ion were to continue forward without transferring its momentum to the compound system, the energy loss to the recoils produced would be less than 10%. It is possible that a consistent 10% decrease in the recoil ranges might be undetected in these experiments.

The slight sensitivity of the parameters T and B/A has already been discussed. The value of $T = 2.5$ Mev was selected by matching information on the experimental excitation function reported by Choppin^{4,5}; this magnitude of temperature agrees reasonably with measured temperatures for neutrons emitted from heavy-ion reactions.²³ The value $B/A = 1.2$ was selected using semiclassical reasoning similar to that of Ericson and Strutinski.⁹ This choice was in reasonable agreement with the experimental results of Knox²⁴ and Broek.²³ Since their experimental studies were made at much higher bombarding energies than used in this work, $B/A = 1.2$ is taken to be an extreme upper limit which will require a minimal E_{γ} . Figure 8 shows that if this value were reduced by a factor of 2 or 3, the calculated angular distribution would broaden by about 0.3 degree and require E_{γ} to be still larger to maintain the fit to experiment.

Figures 2 and 11 show that the recoil angular distributions diverge markedly from the calculated case for isotropic neutron emission and $E_{\gamma} = 0$. This indicates that a significant fraction of the excitation energy is being dissipated by some mechanism other than neutron emission. The

magnitude of this difference greatly exceeds the most conservative estimates of error from all known sources. If the nonisotropic Monte Carlo calculation is used, with B/A fixed as already discussed, a fit to the experiments can be obtained by varying E_γ .

The values required to obtain fits are shown in Table I. They show a gradual increase with excitation energy. Use of E_γ in this way is equivalent to saying the Q of the reaction is larger than its calculated ground-state value. If these Q values adjusted by E_γ are introduced into the Jackson calculation,²¹ the fit to the experimental excitation functions can be maintained by reducing T to about 2 Mev.

Figure 9 shows that a reduction in T by 0.5 Mev would cause the recoil angular distribution to become about 0.3 degree narrower; to compensate for this decrease, E_γ must also decrease by 1.5 Mev. On the other hand, if B/A should decrease to 0.1, there must be a compensating increase of E_γ by about 5 Mev. This shows, therefore, that the magnitude of the effect represented by E_γ does not depend strongly upon the choice of B/A .

The remarkable feature about the excitation function data of Choppin and collaborators is that the maximum cross section occurs at an incident particle energy which is 10 to 15 Mev higher than would be expected from simple theory, assuming an emission of neutrons with an average energy of 3 to 4 Mev. Huizenga has pointed out that most available excitation function data indicate that such neutron energies are to be expected.²⁵

The maximum measured cross section for this reaction is 500 ± 100 mb.⁴

A most interesting problem is to account for the differences between this reaction and the $\text{Pr}^{141}(\text{C}^{12}, 4n)$ reaction. In both cases the bombarding and excitation energies are comparable. However, compound nuclei are

formed with a wide range of spin values. If the $\text{Pr}^{141}(\text{C}^{12}, 4n)\text{Tb}^{149}$ reaction occurs almost exclusively with compound nuclei of low spin, then its behavior should be "normal" and E_{γ} should indeed be zero. In the case of Ce^{137m} , the reverse is true because it was the high-spin (11/2-) isomer which was observed rather than the (3/2+) ground state.

Mollenauer²⁶ has recently reported increased yields of gamma radiation for C^{12} -induced reactions compared to He^4 -induced reactions leading to the same compound nucleus. From measurements of the gamma-ray energy spectra and angular anisotropies with respect to the incident beam, he concludes that the gamma ray cascade occurs mainly through enhanced quadrupole emission from vibrational states.

Using the reaction $\text{La}^{139}(\text{O}^{16}, 6n)\text{Tb}^{149}$ over a bombarding energy range of 80-140 Mev, MacFarlane has recently discovered an isomeric state of Tb^{149} which is considered to have a spin of 11/2, compared with 5/2 for Tb^{149g} . Since the excitation function for the formation of the isomer was found to be displaced to about 10 Mev higher energy than that for formation of the ground state, it seems probable that the two are indeed formed from the high- and low-spin states of the compound nucleus, respectively. The Tb^{149m} was found to decay partially through the ground state. In our study of Tb^{149g} produced by the reaction $\text{Pr} + \text{C}$, the extent of complication due to possible formation of the isomeric state is uncertain. There is no apparent displacement of the excitation function; use of a less massive ion and a lower range of bombarding energies might have reduced any contribution from the isomeric state, if it is formed at all.

As a result of Mollenauer's work, Choppin's and MacFarlane's excitation functions, and the present experiments, it now seems firmly established that an enhancement in the yield of gamma radiation is a common feature of heavy-ion-induced nuclear reactions.

ACKNOWLEDGMENTS

We wish to thank the crew of the HILAC for their assistance with the various experiments. We are particularly grateful to Drs. John O. Rasmussen, John R. Huizenga, John M. Alexander, Ronald D. MacFarlane, and James F. Mollenauer for valuable discussions and suggestions during the course of this work.

REFERENCES

*Work done under the auspices of the U. S. Atomic Energy Commission.

†Present address: University of California Lawrence Radiation Laboratory, Livermore, California.

‡Part of this work was submitted in partial fulfillment of the requirements of the Ph. D. degree in chemistry at the University of California, Berkeley, California.

§Present address: Florida State University, Tallahassee, Florida.

¹P. F. Donovan, B. G. Harvey, and W. H. Wade, Phys. Rev. 119, 218 (1960).

²B. G. Harvey, W. H. Wade, and P. F. Donovan, Phys. Rev. 119, 225 (1960).

³J. R. Morton and B. G. Harvey, Phys. Rev. (to be published).

⁴G. R. Choppin and T. Klingen, Florida State University, Tallahassee, Florida (unpublished data).

⁵G. R. Choppin, "Research in Nuclear Chemistry, Progress Report, June 1, 1959 - May 31, 1960," Florida State University, Tallahassee, Florida (unpublished).

⁶J. R. Walton, Lawrence Radiation Laboratory, Berkeley (unpublished data).

⁷L. C. Northcliffe, Phys. Rev. 120, 1744 (1960).

⁸B. P. Bayhurst and R. J. Prestwood, Nucleonics 17, No. 3, 82 (1959).

⁹T. Ericson and V. Strutinski, Nuclear Phys. 8, 284 (1958); with corrections from Nuclear Phys. 9, 689 (1959).

¹⁰I. Halpern and V. Strutinski, Proc. U. N. Intern. Conf. Peaceful Uses Atomic Energy, 2nd, Geneva, 1958, Vol. 15 (United Nations, Geneva, 1958).

¹¹G. A. Pik-Pichak, Soviet Phys. JETP 11, 557 (1960); J. Exptl. Theoret. Phys. (U. S. S. R.) 38, 768 (1960).

¹²K. J. Le Couteur, Nuclear Reactions, Vol. 1, P. M. Endt and M. Demeur, Eds. (North-Holland Publishing Co., Amsterdam, 1959).

¹³K. J. Le Couteur and D. W. Lang, Nuclear Phys. 13, 32 (1959).

¹⁴D. W. Lang and K. J. Le Couteur, Proc. Phys. Soc. (London) 67A, 585 (1954).

¹⁵The angles given here are determined by the mean radii of the catcher foil rings and a 4.0-cm target-to-catcher distance. The angular increments intercepted by the successive rings are: 4.64, 2.66, 2.82, 2.70, 2.88, 2.42, 2.56, 2.40, 2.38, 2.26, and 2.10 degrees. These increments correspond to spherical zones of relative area: 1.00, 1.48, 2.29, 2.81, 3.79, 3.76, 4.56, 4.77, 5.20, 5.38, and 5.68.

¹⁶The angles given here are determined by the mean radii of the catcher foil rings and a 6.0-cm target-to-catcher distance. The angular increments intercepted by the successive rings are: 3.08, 1.80, 1.90, 1.84, 1.96, 1.68,

1.92, 1.76, 1.72, 1.70, and 1.60 degrees. These increments correspond to spherical zones of relative area: 1.00, 1.47, 2.22, 2.84, 3.95, 3.94, 4.83, 5.37, 5.75, 6.29, and 6.45.

¹⁷J. M. Alexander and L. Winsberg, Phys. Rev. 121, 529 (1961).

¹⁸B. G. Harvey, Ann. Revs. Nuclear Sci. 10, 235 (1960). (E. Segré, Editor, Annual Reviews, Inc., Palo Alto, Calif.)

¹⁹L. Winsberg and J. M. Alexander, Phys. Rev. 121, 518 (1961).

²⁰J. Lindhard and M. Scharff, Phys. Rev. 124, 128 (1961).

²¹J. M. Alexander, Lawrence Radiation Laboratory, Berkeley (unpublished data).

²²J. D. Jackson, Can. J. Phys. 34, 767 (1956).

²³H. W. Broek, "Neutron Emission from Compound Systems of High Angular Momentum," Ph. D. thesis, Yale University, 1960 (unpublished).

²⁴W. J. Knox, Proceedings of the Second Conference on Reactions Between Complex Nuclei (John Wiley & Sons, Inc., New York, 1960).

²⁵J. R. Huizenga, Argonne National Laboratory, Lemont, Ill. (private communication).

²⁶J. F. Mollenauer, "Effects of Angular Momentum on Gamma Ray Production in Compound Nucleus Reactions," Ph. D. thesis, Univ. Calif., Berkeley. Lawrence Radiation Laboratory (Berkeley) Rept. UCRL-9724, June, 1960 (unpublished).

²⁷R. D. MacFarlane, Phys. Rev. Letters (to be published).

Table I. Summary of parameters for best fit of calculated recoil angular distributions to experiment - $\text{Te}^{130}(\text{C}^{12}, 5n)\text{Ce}^{137m}$.

$E_{\text{C}^{12}}$ (Mev)	T = 2.5 Mev E_{γ} (Mev)	T = 1.5 Mev E_{γ} (Mev)
59.0	5	5
64.5	6	6
69.0	7	8
75.0	8	8
81.0	11	8
87.5	15	11

Table II. Summary of experimental recoil angular distribution data - $\text{Te}^{130}(\text{C}^{12}, 5n)\text{Ce}^{137m}$.

$E_{\text{C}^{12}}$ (Mev)	$W(1/2)^a$ (deg)	Relative $d\sigma/d\Omega$, for angles in degrees									
		1.54^b	3.99	5.84	7.70	9.61	11.44	13.20	14.97	16.71	18.44
59.0	4.5	59^c	23	14.5	9.5	4.1	2.6	1.4	1.0	0.78	0.52
64.5	5.6	67^d	49	36	14	6.8	4.0	1.7	0.78	0.38	
69.0	5.2	17^e	12.5	7.2	4.5	2.4	1.5	1.1	0.65	0.40	0.39
81.0	6.0	64^e	48	36	24	12.5	8.5	5.0	4.2	4.8	
87.5	6.2	52^e	37	29	21	11	11	8.5	4.5	6.7	5.2
		2.31^f	5.97	8.71	11.47	14.24	16.88	19.38	21.85	24.23	
74.5	5.8	51^g	27	14	9.5	3.5	2.5	2.0	1.3		

^aThe overall error in $W(1/2)$ is estimated to be $\leq \pm 0.5\%$.

^bSee footnote 16.

^cOverall errors are estimated to be $\leq 5\%$ to 9.61 deg.

^dOverall errors are estimated to be $\leq 3\%$ to 9.61 deg.

^eOverall errors are estimated to be $\leq 6\%$ to 7.70 deg.

^fSee footnote 15.

^gOverall errors are estimated to be $\leq 4\%$.

Table III. Summary of natural Te + C¹² recoil range data.

$E_{C^{12}}$ (Mev)	E_r (Mev)	Group	R_0 from Tb ¹⁴⁹		ρ Exptl.	ρ Theoret.	Exptl. σ ($\mu\text{g}/\text{cm}^2$)
			Exptl. R_0 ($\mu\text{g}/\text{cm}^2$ Al)	data ($\mu\text{g}/\text{cm}^2$ Al)			
70	5.40	Long-lived	428	493	0.339	0.304	145
		Short-lived	435	493	0.333	0.304	145
80.3	6.20	Long-lived	475	554	0.280	0.304	133
		Short-lived	482	554	0.276	0.304	133
90	6.95	Long-lived	580	610	0.279	0.304	162
		Short-lived	580	610	0.279	0.304	162
99.5	7.70	Long-lived	580	660	0.283	0.304	164
		Short-lived	590	660	0.276	0.304	163

Table IV. Summary of experimental recoil angular distribution data —
 $\text{Pr}^{141}(\text{C}^{12}, 4n)\text{Tb}^{149}$.

$E_{\text{C}^{12}}$ (Mev)	$W(1/2)^a$ (deg)	Relative $d\sigma/d\Omega$, for angles in degrees ^b								
		1.54	3.99	5.84	7.70	9.61	11.44	13.20	14.97	16.71
58.0	4.8	92 ^c	61	36	16	5.4	1.9	0.8	0.27	
61.5	5.0	95 ^d	66	39	19	6.2	2.3	0.9	0.43	
64.5	5.1	94 ^c	70	38	20	6.4	2.8	0.7	0.3	
69.5	5.2	95 ^d	68	42	22	6.2	2.7	0.9	0.4	
71.5	5.8	94 ^c	70	49	29	10	5.7	1.8	1.1	0.5

^aThe overall error in $W(1/2)$ is estimated to be $\leq \pm 0.5\%$.

^bSee footnote 16.

^cErrors due to counting statistics are $\leq 6\%$ to 7.70 deg.

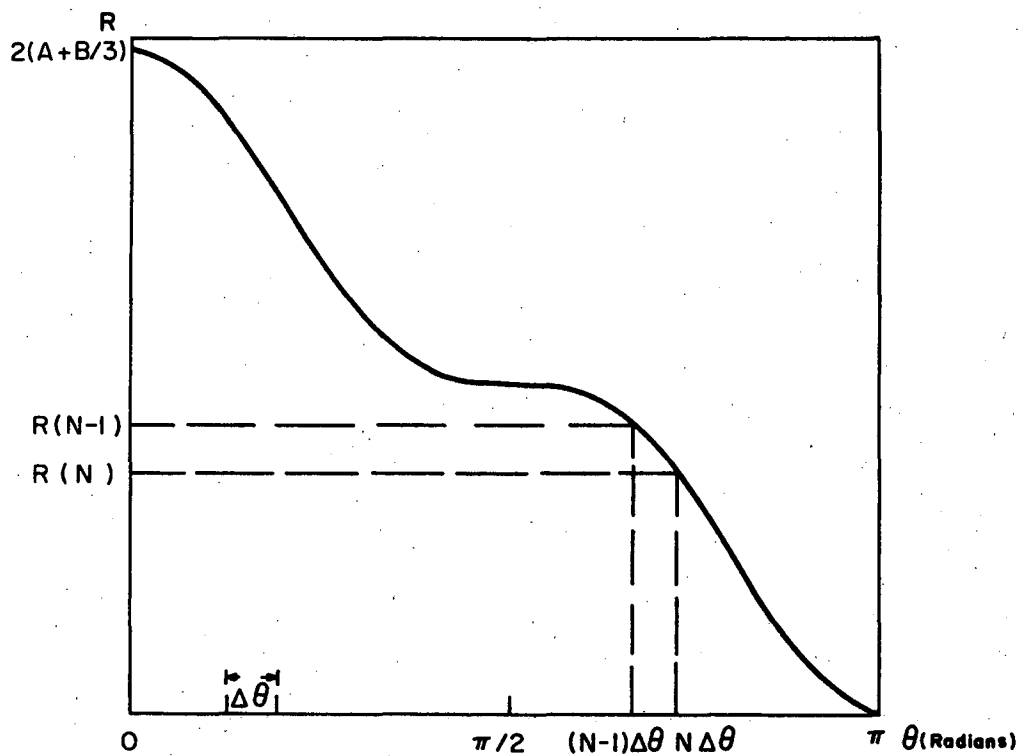
^dErrors due to counting statistics are $\leq 3\%$ to 7.70 deg.

FIGURE CAPTIONS

- Fig. 1. The integral probability function for selection of the polar angle θ . The scales are greatly expanded.
- Fig. 2. Comparison of calculated (smooth curves and dashed curves) and experimental (points) recoil angular distributions for the system $\text{Te}^{130}(\text{C}^{12}, 5n)\text{Ce}^{137m}$. The smooth curves are calculated with $B/A = 1.2$, $T = 2.5$ Mev, and E_{γ} as a free parameter; the dashed curves are calculated for isotropic neutron emission, $T = 2.5$ Mev, and $E_{\gamma} = 0$. All the distributions begin at 0 degrees but are displaced in the figure with no change in scale.
- Fig. 3. Comparison between calculated (smooth curves) and experimental (points) recoil angular distributions for the reaction $\text{Pr}^{141}(\text{C}^{12}, 4n)\text{Tb}^{149}$. All the distributions begin at 0 degrees, but are displaced in the figure with no change in scale.
- Fig. 4. Plot of the neutron angular distribution $W(\theta) = A + B \cos^2 \theta$ in the system of the recoiling nucleus for $B/A = 100$. The dotted line is the actual distribution; the solid lines are the histogram from the mesh size; the dashed line is obtained by integrating the histograms; points are from the computations.
- Fig. 5. Plot of the neutron angular distributions for various values of B/A : (1) 10^{-10} , (2) 1, (3) 10, (4) 100.
- Fig. 6. Calculated neutron energy spectra for the reaction $\text{Pb}^{208}(\alpha, 2n)\text{Po}^{210}$, $T = 1.45$ Mev and $E_{\alpha(\text{c. m.})} + Q_2 =$ (a) 5.1 Mev, (b) 8.7 Mev, and (c) 12.9 Mev.
- Fig. 7. Calculated neutron energy spectra for the reaction $\text{Te}^{130}(\text{C}^{12}, 5n)\text{Ce}^{137}$, $T = 2.5$ Mev, $E_{\gamma} = 5.0$ Mev, and $E_{\text{C}^{12}} + Q_5 =$ (a) 18 Mev, (b) 28 Mev, and (c) 39 Mev.

FIGURE CAPTIONS (Cont'd)

- Fig. 8. The variation of $W(1/2)$ as a function of the ratio B/A .
- Fig. 9. Plot of the magnitude of the angle $W(1/2)$ at which the relative differential cross section is reduced to half the forward value, as a function of nuclear temperature.
- Fig. 10. Plot of the magnitude of the angle $W(1/2)$ at which the relative differential cross section is reduced to half the forward value, as a function of E_{γ} for the reaction $\text{Te}^{130}(\text{C}^{12}, 5n)\text{Ce}^{137}$. $E_{\text{C}^{12}} = 75$ Mev, $T = 2.5$ Mev.
- Fig. 11. Plot of $W(1/2)$ vs $E_{\text{C}^{12}(\text{c. m.})} + Q$ for $\text{Te}^{130}(\text{C}^{12}, 5n)\text{Ce}^{137\text{m}}$. Solid line is fitted to experimental points. Dotted line fits the case for $B/A \rightarrow 0$, $E_{\gamma} = 0$ (isotropic case).
- Fig. 12. Histogram for the ranges of the recoiling Ce and La products of natural $\text{Te} + \text{C}^{12}$ at $E_{\text{C}^{12}} = 90$ Mev. The solid lines indicate the long-lived group; the dashed lines indicate the short-lived group.
- Fig. 13. Probability plot of Ce and La recoil ranges in aluminum for $E_{\text{C}^{12}} = 90$ Mev. The points $-\sigma$, $+\sigma$, and R_0 are indicated. In this case $R_0 = 580 \mu\text{g}/\text{cm}^2$ and $\sigma = 162 \mu\text{g}/\text{cm}^2$.
- Fig. 14. Range-energy curve for the recoiling Ce and La products from the reactions of natural $\text{Te} + \text{C}^{12}$. The experimental points are compared with a solid curve calculated from the Tb^{149} range of ref. 19.
- Fig. 15. Plot of $W(1/2)$ versus $E_{\text{C}^{12}(\text{c. m.})} + Q$ for $\text{Pr}^{141}(\text{C}^{12}, 4n)\text{Tb}^{149}$.



MU-23034

Fig. 1. The integral probability function for selection of the polar angle θ . The scales are greatly expanded.

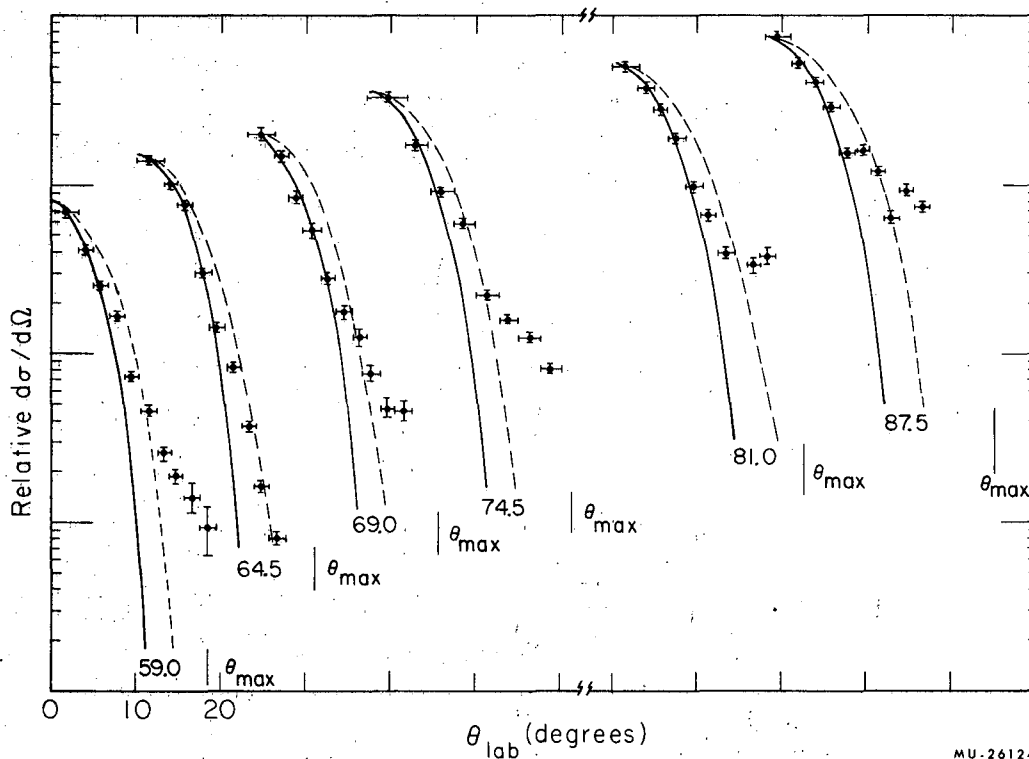


Fig. 2. Comparison of calculated (smooth curves and dashed curves) and experimental (points) recoil angular distributions for the system $\text{Te}^{130}(\text{C}^{12}, 5n)\text{Ce}^{137m}$. The smooth curves are calculated with $B/A = 1.2$, $T = 2.5$ Mev, and E_{γ} as a free parameter; the dashed curves are calculated for isotropic neutron emission, $T = 2.5$ Mev, and $E_{\gamma} = 0$. All the distributions begin at 0 degrees but are displaced in the figure with no change in scale.

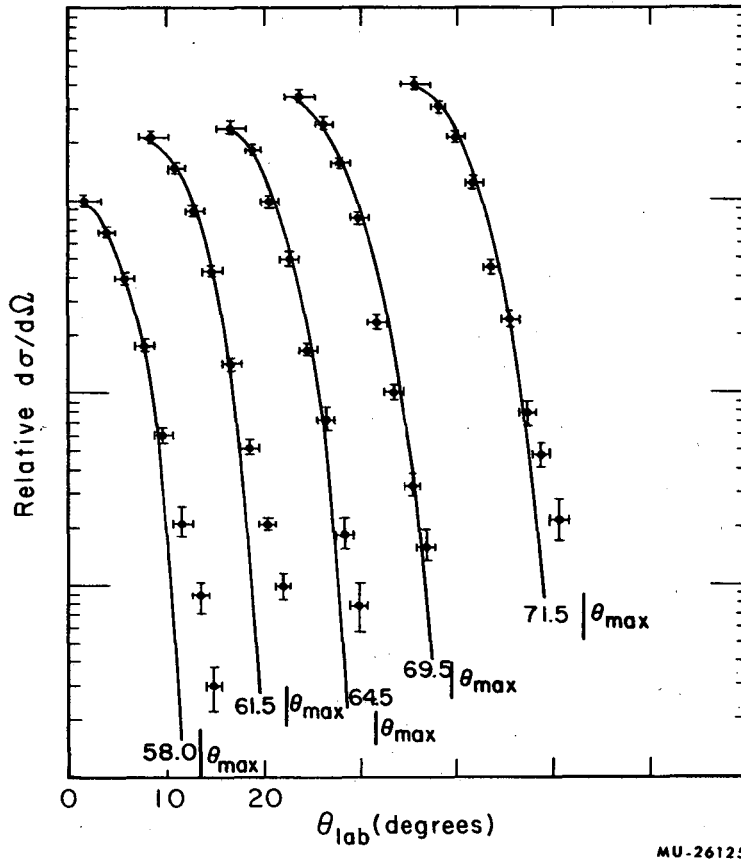
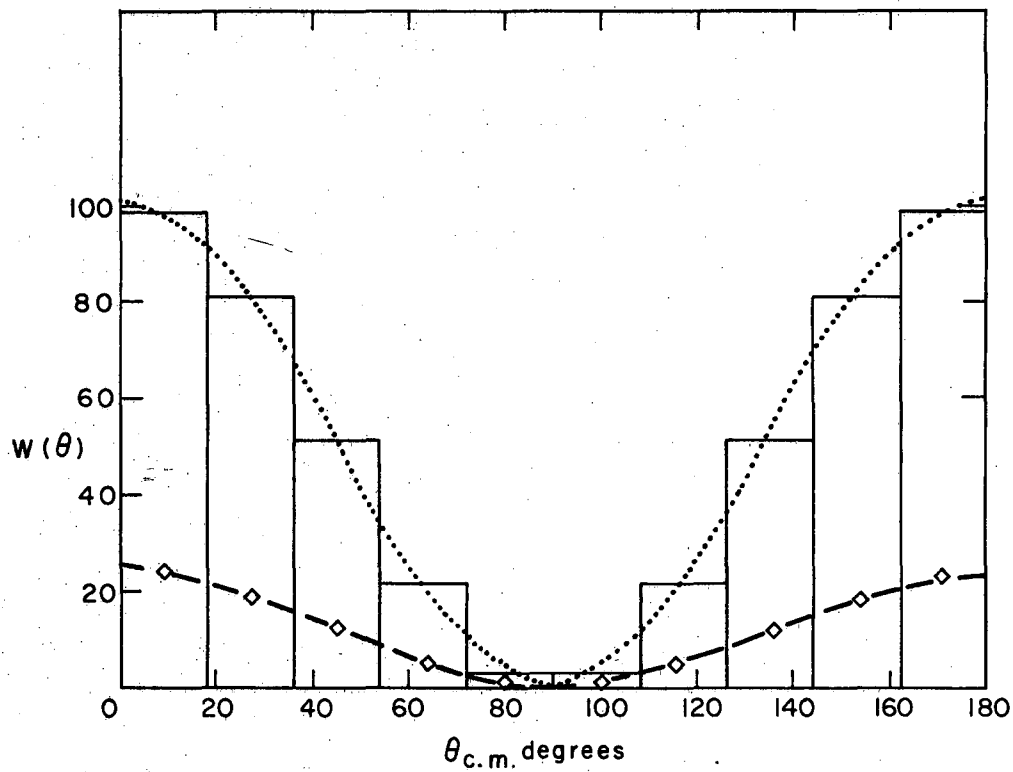
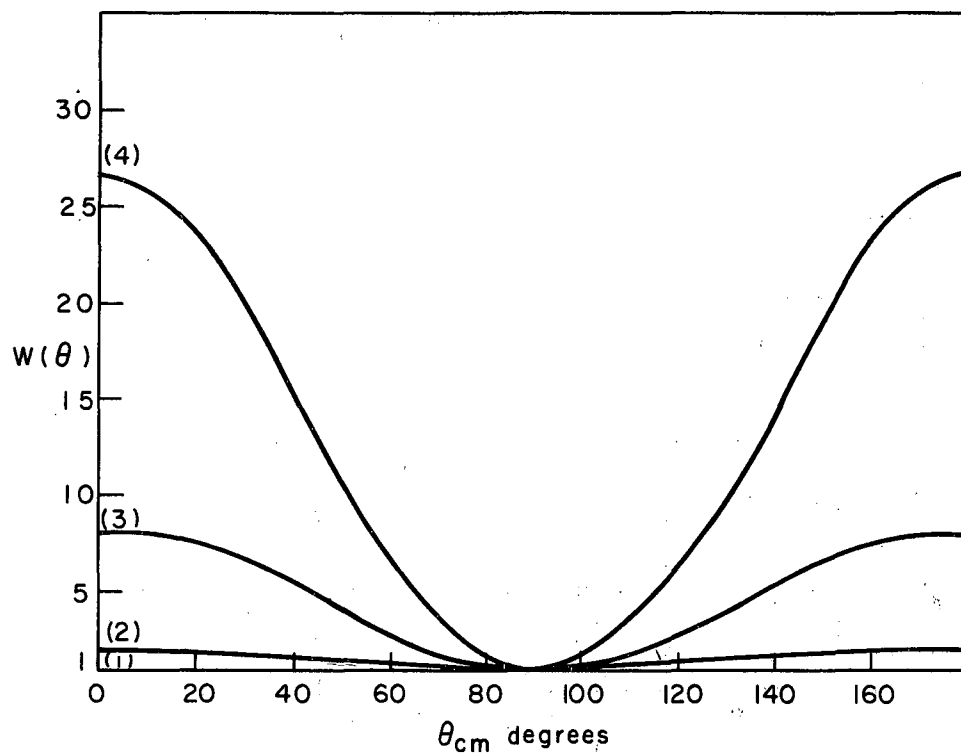


Fig. 3. Comparison between calculated (smooth curves) and experimental (points) recoil angular distributions for the reaction $Pr^{141}(C^{12}, 4n)Tb^{149}$. All the distributions begin at 0 degrees, but are displaced in the figure with no change in scale.



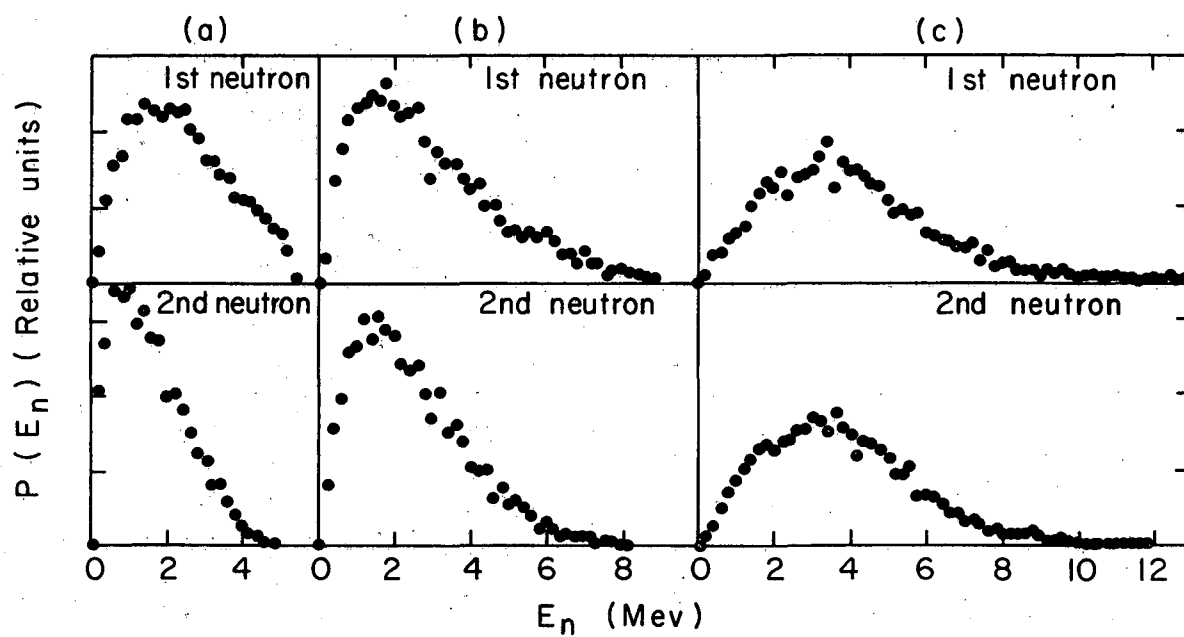
MU-23035

Fig. 4. Plot of the neutron angular distribution $W(\theta) = A + B \cos^2 \theta$ in the system of the recoiling nucleus for $B/A = 100$. The dotted line is the actual distribution; the solid lines are the histogram from the mesh size; the dashed line is obtained by integrating the histograms; points are from the computations.



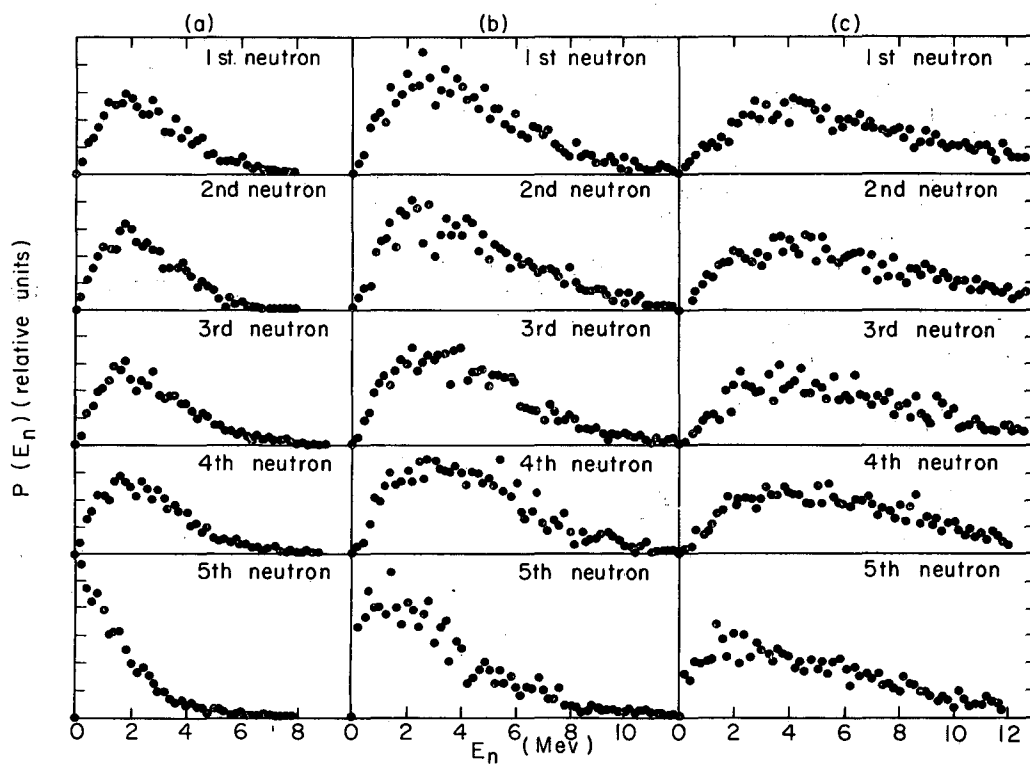
MU-23036

Fig. 5. Plot of the neutron angular distributions for various values of B/A : (1) 10^{-10} , (2) 1, (3) 10, (4) 100.



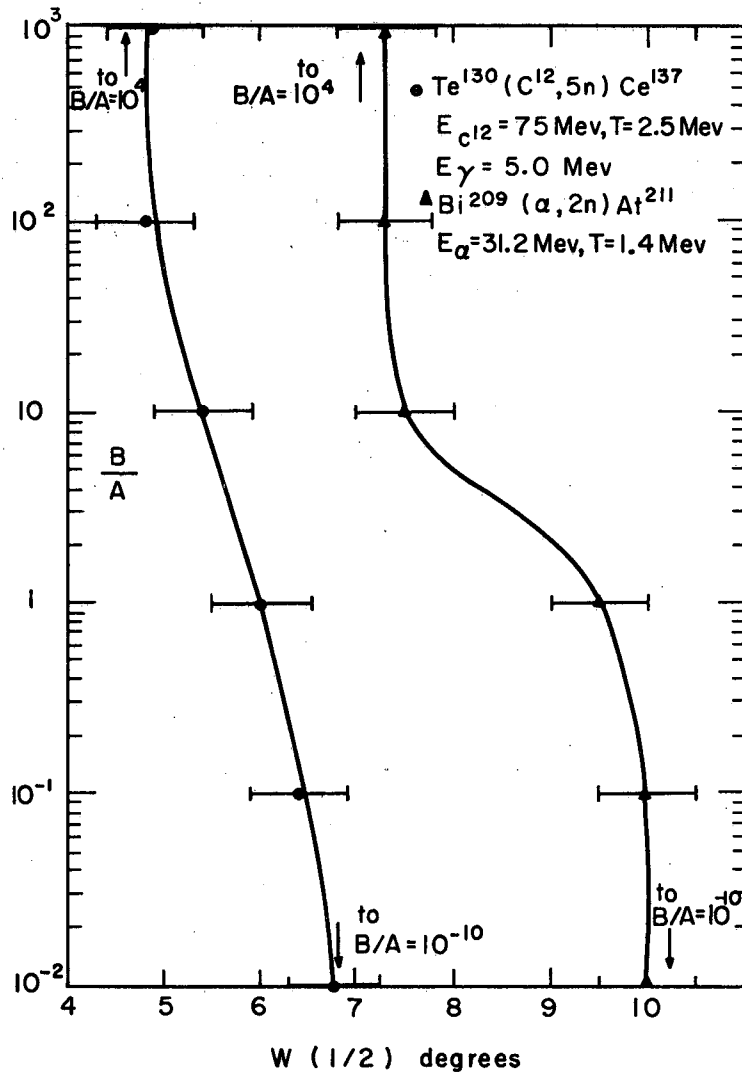
MU-23037

Fig. 6. Calculated neutron energy spectra for the reaction $\text{Pb}^{208}(\alpha, 2n)\text{Po}^{210}$, $T = 1.45$ Mev and $E_{a(c.m.)} + Q_2 =$ (a) 5.1 Mev, (b) 8.7 Mev, and (c) 12.9 Mev.



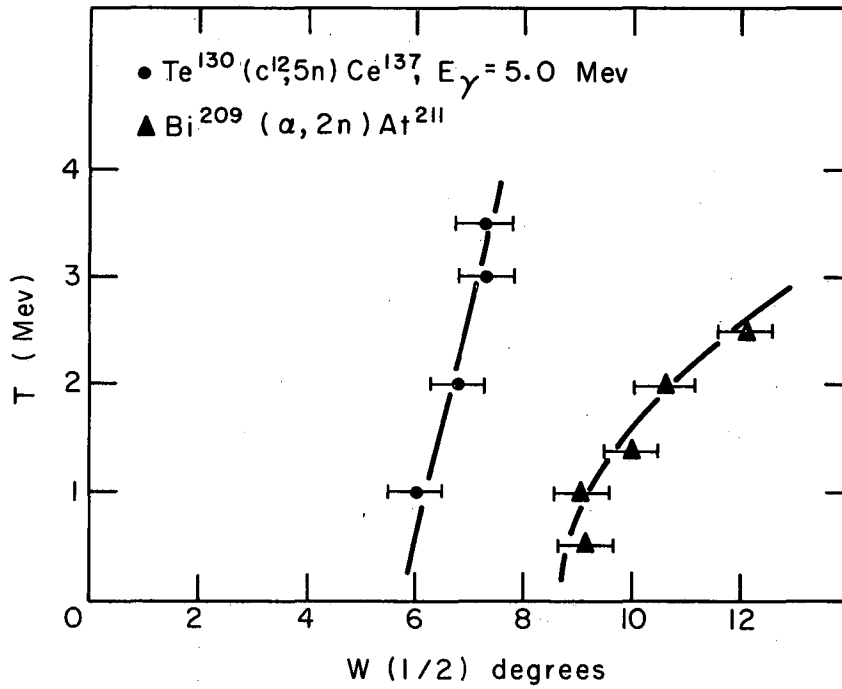
MU-23038

Fig. 7. Calculated neutron energy spectra for the reaction $\text{Te}^{130}(\text{C}^{12}, 5n)\text{Ce}^{137}$, $T = 2.5$ Mev, $E_{\gamma} = 5.0$ Mev, and $E_{\text{C}^{12}} + Q_5 =$ (a) 18 Mev, (b) 28 Mev, and (c) 39 Mev.



MU-23033

Fig. 8. The variation of $W(1/2)$ as a function of the ratio B/A .



MU-23029

Fig. 9. Plot of the magnitude of the angle $W(1/2)$ at which the relative differential cross section is reduced to half the forward value, as a function of nuclear temperature.

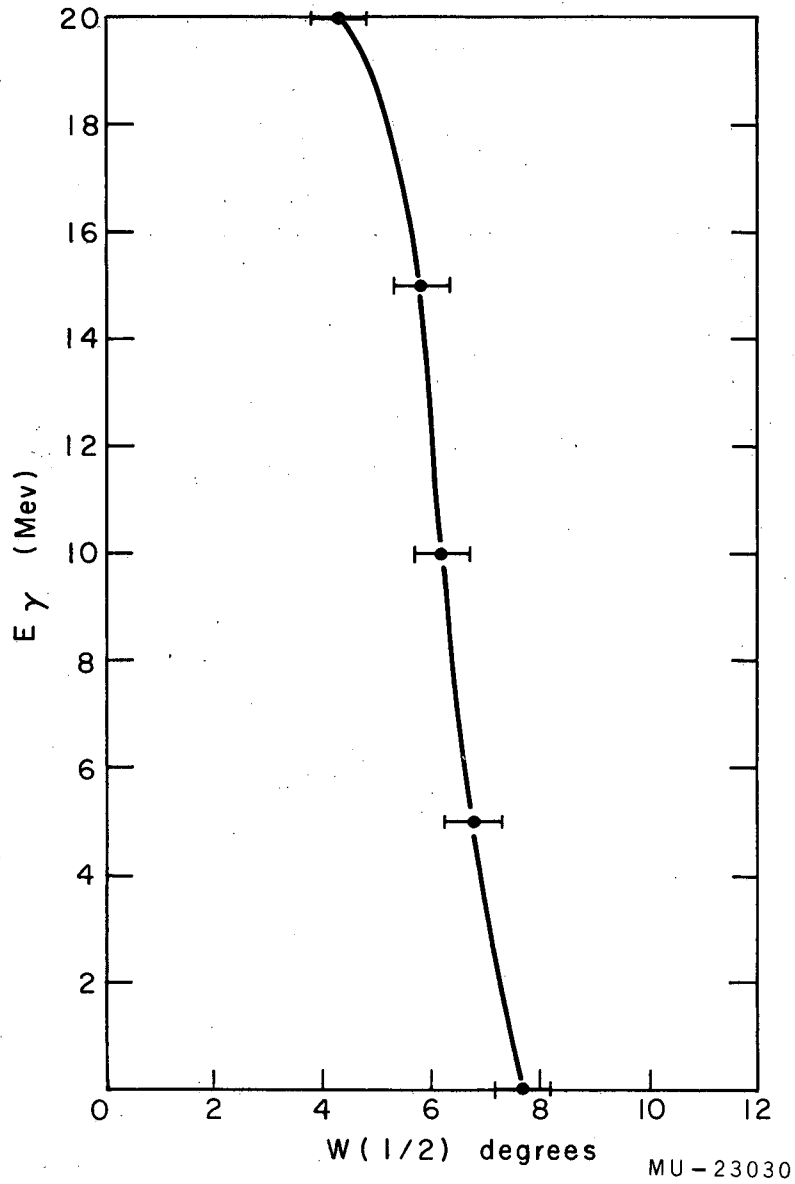
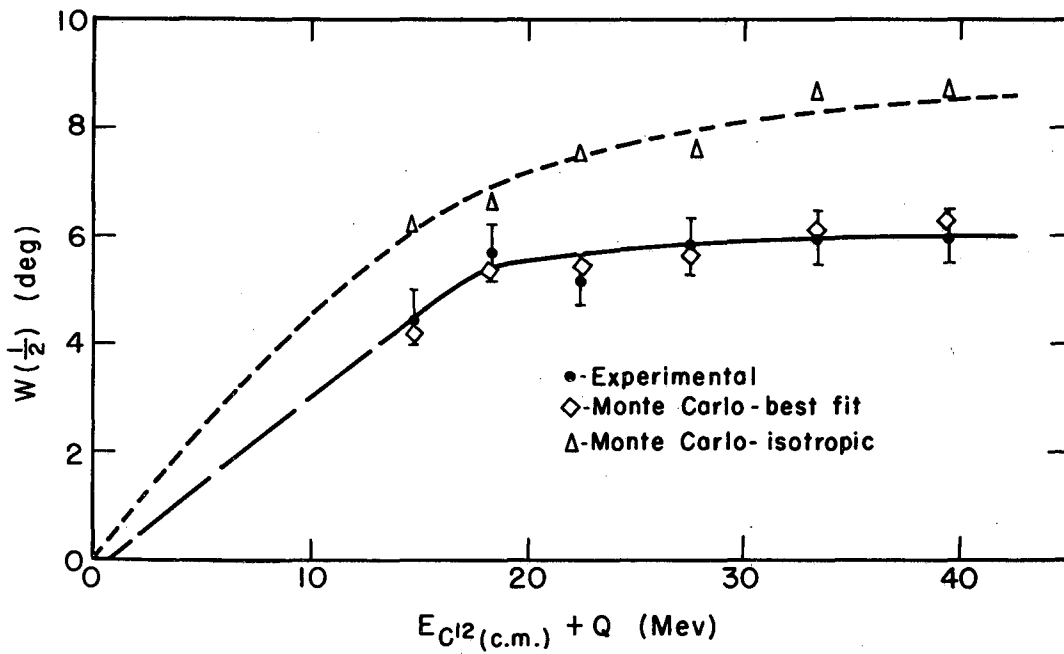
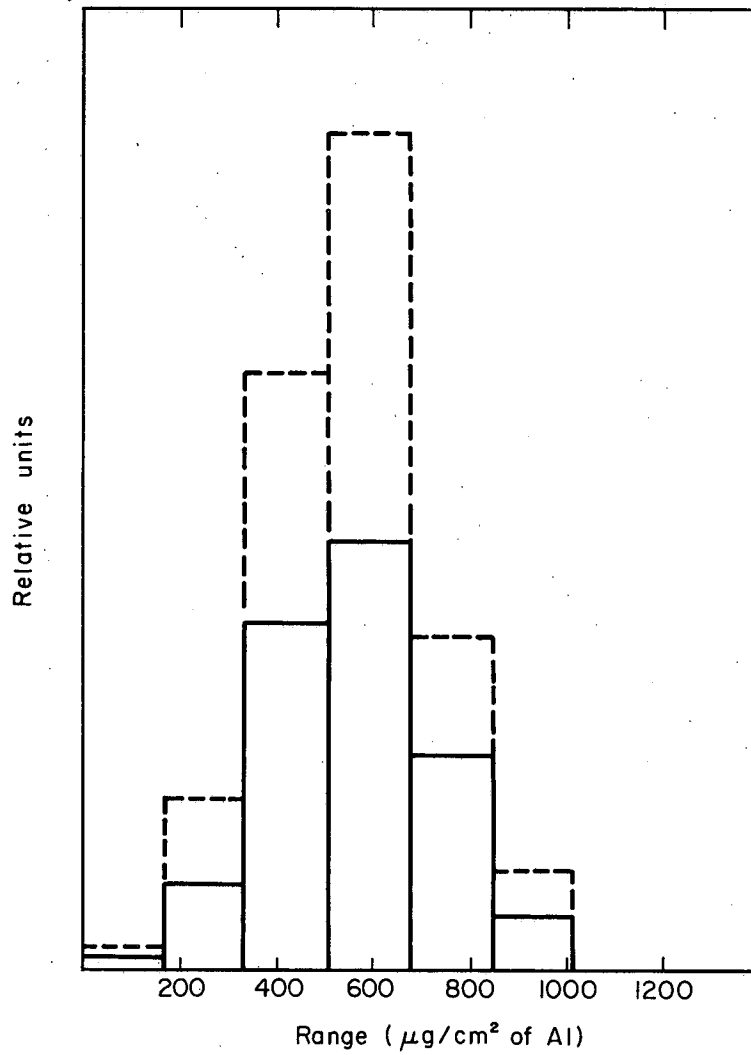


Fig. 10. Plot of the magnitude of the angle $W(1/2)$ at which the relative differential cross section is reduced to half the forward value, as a function of E_γ for the reaction $Te^{130}(C^{12}, 5n)Ce^{137}$. $E_{C^{12}} = 75$ Mev, $T = 2.5$ Mev.



MU-23454

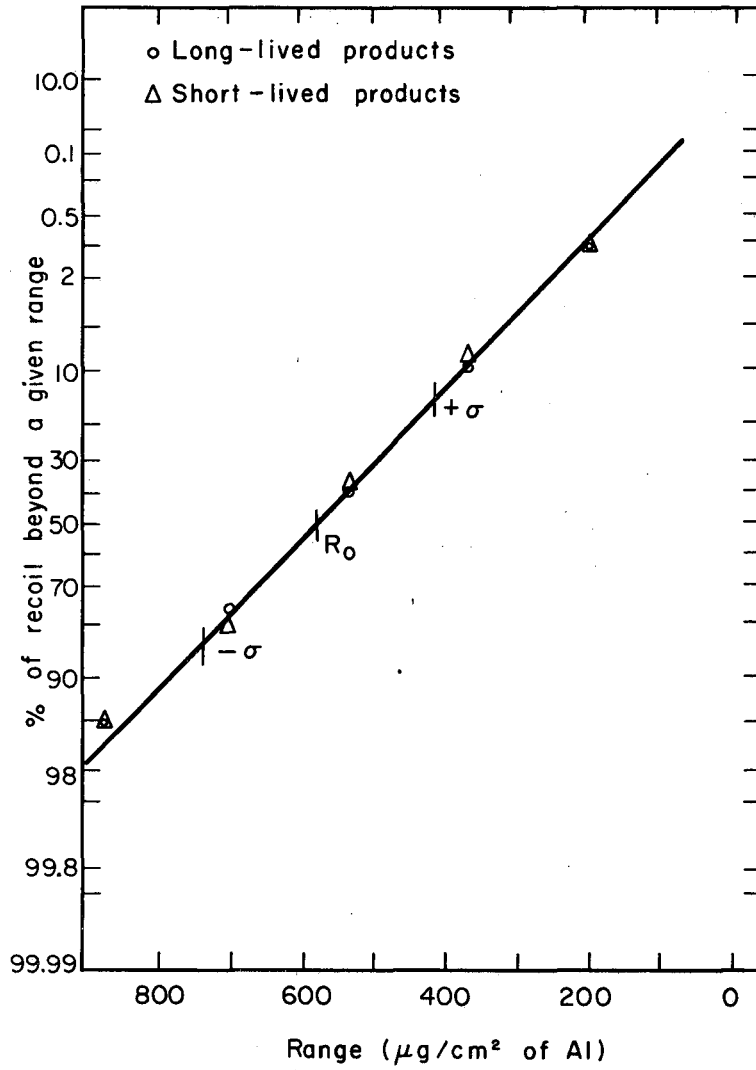
Fig. 11. Plot of $W(1/2)$ vs $E_{C^{12}(c.m.)} + Q$ for $Te^{130}(C^{12}, 5n)Ce^{137m}$. Solid line is fitted to experimental points. Dotted line fits the case for $B/A \rightarrow 0$, $E_{\gamma} = 0$ (isotropic case).



MU-23046

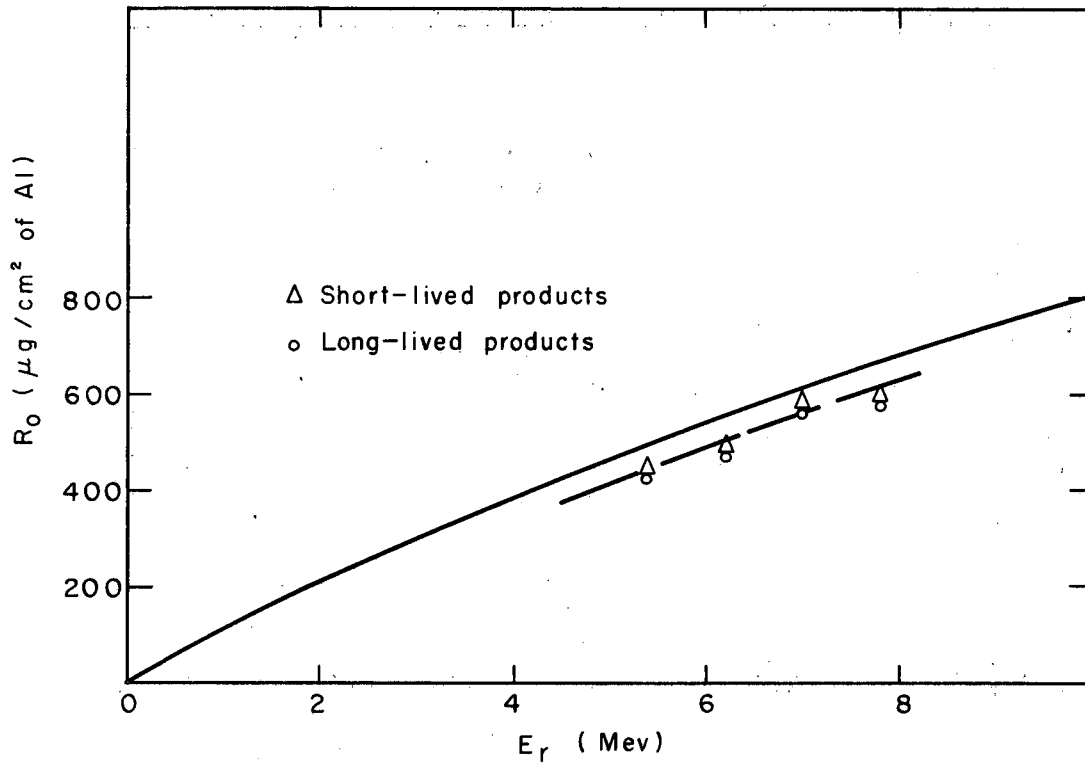
Fig. 12. Histogram for the ranges of the recoiling Ce and La products of natural Te + C¹² at E_{C¹²} = 90 Mev.

The solid lines indicate the long-lived group; the dashed lines indicate the short-lived group.



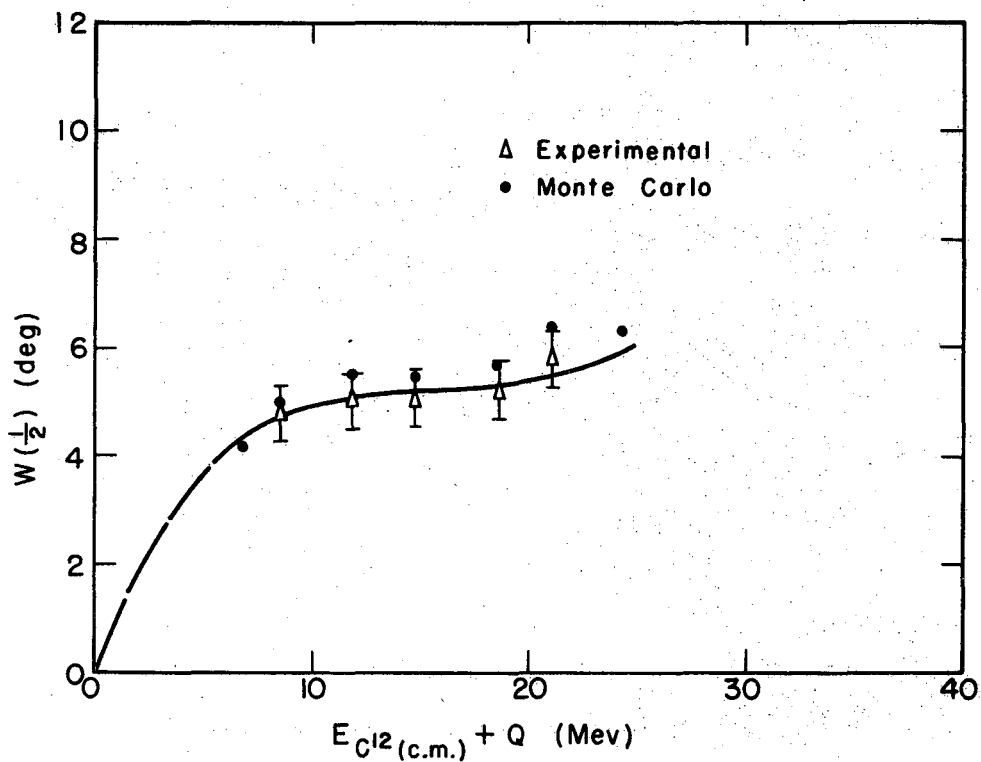
MU-23047

Fig. 13. Probability plot of Ce and La recoil ranges in aluminum for $E_{C^{12}} = 90$ Mev. The points $-\sigma$, $+\sigma$, and R_0 are indicated. In this case $R_0 = 580 \mu\text{g}/\text{cm}^2$ and $\sigma = 162 \mu\text{g}/\text{cm}^2$.



MU-23048

Fig. 14. Range-energy curve for the recoiling Ce and La products from the reactions of natural Te + Cl^{32} . The experimental points are compared with a solid curve calculated from the Tb^{149} range of ref. 19.



MU-23455

Fig. 15. Plot of $W(1/2)$ versus $E_{C^{12}(c.m.)} + Q$
for $Pr^{141}(C^{12}, 4n) Tb^{149}$.

This report was prepared as an account of Government sponsored work. Neither the United States, nor the Commission, nor any person acting on behalf of the Commission:

- A. Makes any warranty or representation, expressed or implied, with respect to the accuracy, completeness, or usefulness of the information contained in this report, or that the use of any information, apparatus, method, or process disclosed in this report may not infringe privately owned rights; or
- B. Assumes any liabilities with respect to the use of, or for damages resulting from the use of any information, apparatus, method, or process disclosed in this report.

As used in the above, "person acting on behalf of the Commission" includes any employee or contractor of the Commission, or employee of such contractor, to the extent that such employee or contractor of the Commission, or employee of such contractor prepares, disseminates, or provides access to, any information pursuant to his employment or contract with the Commission, or his employment with such contractor.